Transactions of Tianjin University (2020) 26:256–264
https://doi.org/10.1007/s12209-020-00256-6

RESEARCH ARTICLE

Nano-silica-decorated Poly(*m*-Phenylene Isophthalamide) Separator with Enhanced Mechanical and Electrolyte Wetting Properties for Lithium-Ion Batteries

Jianjie Wang[1,3] · Biao Yuan[2] · Fusheng Pan[1,3] · Lina Qiao[1,3] · Jun Guo[2] · Cuijia Duan[2] · Wei Wu[2] · Zan Chen[2] · Yanlei Su[1,3]

Received: 4 April 2020 / Revised: 29 April 2020 / Accepted: 13 May 2020 / Published online: 3 June 2020

Abstract

Heat-resistant poly(*m*-phenylene isophthalamide) (PMIA) has attracted considerable attention as a novel separator for application in lithium-ion batteries (LIBs); however, its mechanical strength and electrolyte wettability are not ideal. Herein, a nano-silica-decorated poly(*m*-phenylene isophthalamide) (PMIA@SiO_2) separator was fabricated with SiO_2 nanoparticles uniformly attached to the pores and pore walls of the PMIA separator. The as-prepared PMIA@SiO_2 separator has good mechanical strength (a 16% improvement compared with pristine PMIA) and wettability toward the electrolyte (the contact angle decreases from 34.0° to 23.1°). The PMIA@SiO_2 separator also had a high ionic conductivity (0.75 mS/cm) and low interfacial electric resistance (75 Ω). The assembled $LiCoO_2$/PMIA@SiO_2-liquid electrolyte/Li cell displays good cycle performance with a capacity retention of 88.1% after 50 cycles. Furthermore, the cycling performance and rate capacity rarely changed after high-temperature treatment. Therefore, the nano-silica-decorated PMIA separator is a potential candidate for application in LIBs with high safety.

Keywords Li-ion batteries · PMIA@SiO_2 Separator · Mechanical strength · Electrolyte wetting

Introduction

Lithium-ion batteries (LIBs) are widely used in portable electronic devices and electric vehicles [1, 2]. The separator is an indispensable component of the LIB system that can impede the short circuit between positive and negative electrodes to guarantee the safety of batteries [3]. Most separators in LIBs are polyolefin owing to their good chemical stability and robust mechanical strength [4]. Nevertheless, there are limitations in their use in LIBs due to inferior thermal stability, poor wettability, and low porosity [5]. Therefore, many studies have used inorganic materials (Al_2O_3) [6, 7] and high heat-resistant polymers [8–10] to replace polyolefin separators. Wang et al. [11] fabricated a paper-supported inorganic composite separator with high thermal stability, and the resulting battery exhibited good cyclic and rate performances. Kang et al. [12] manufactured microporous poly(*m*-phenylene isophthalamide) (PMIA) with high thermal stability and excellent flame resistance properties via a conventional, non-solvent-induced phase separation method.

PMIA is a widely used high-temperature-resistant material possessing extremely high heat resistance (up to 400 °C), excellent self-extinguishment, and high chemical corrosion resistance [13–15], and has drawn considerable attention as a novel separator for application in LIBs [16, 17]. PMIA separators currently used for LIBs are typically prepared by the electrospinning method and phase inversion [4, 18,

Electronic supplementary material The online version of this article (https://doi.org/10.1007/s12209-020-00256-6) contains supplementary material, which is available to authorized users.

✉ Zan Chen
chenzan_ac@163.com

✉ Yanlei Su
suyanlei@tju.edu.cn

[1] Key Laboratory for Green Chemical Technology of Ministry of Education, School of Chemical Engineering and Technology, Tianjin University, Tianjin 300072, China

[2] CenerTech Tianjin Chemical Research and Design Institute Co., Ltd, Tianjin 300131, China

[3] Collaborative Innovation Center of Chemical Science and Engineering (Tianjin), Tianjin 300072, China

19]. The separator prepared by electrospinning has many advantages, such as a large number of interconnected holes and a high specific surface area [20, 21]. Nevertheless, the phase inversion method is more suitable given the facility of the process and scalability.

The mechanical strength and wettability of the separator toward electrolytes are essential factors in LIBs, which can influence the internal resistance and ionic conductivity, consequently affecting the safety and cycle performance of the battery. However, the as-obtained separator shows interior performance in LIB applications because of inherent drawbacks of the PMIA separator toward the electrolyte, including low mechanical strength and poor wettability [4, 16]. To overcome the above barriers, previous studies that modified separators with nanoparticles [10, 22, 23], such as SiO_2 [24], Al_2O_3 [25], and polyhedral oligomeric silsesquioxane [4, 26], were used to improve the mechanical strength, electrolyte wettability, and corresponding cell performance. Among them, SiO_2 nanoparticles have a high concentration of hydroxyl groups on their surface, which facilitates the fast absorption of large amounts of liquid electrolytes and efficiently reduces the interfacial resistance between separators and electrodes [27, 28]. Moreover, the preparation process is mild and the particle size is adjustable. Wang et al. [29] fabricated a polyimide (PI) nanofiber separator embedded with SiO_2 nanoparticles and the separator exhibited excellent electrolyte wettability. Therefore, the performance of PMIA separators in LIBs could be enhanced by decorating with SiO_2 nanoparticles. However, nano-silica nanoparticles, which possess a high surface energy and easily aggregate into large grains, are difficult to uniformly disperse in the separator [30–32], leading to interface defects and thus a decrease in the mechanical strength. Moreover, most of the SiO_2 nanoparticles decorate the surface of the separator, while very few studies report the SiO_2 nanoparticles have decorated both the pore wall and surface to improve the mechanical strength and electrolyte wettability of a separator.

In this study, a PMIA separator with uniformly decorated SiO_2 nanoparticles (abbreviated as PMIA@SiO_2) was prepared for LIBs. Pristine PMIA was fabricated by a facile phase inversion method and then homogeneously decorated with SiO_2 nanoparticles using Tween-80 as the dispersion auxiliary. Importantly, the decorating process is binder-free. In addition, the mechanical, electrolyte wetting properties, and corresponding batteries performance of the PMIA@SiO_2 separator were compared with those of the pristine PMIA separator, and the application of the PMIA@SiO_2 separator in LIBs was evaluated.

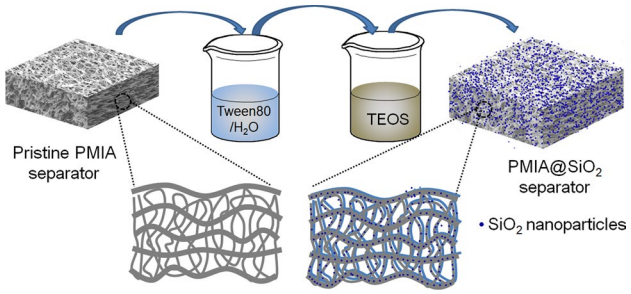

Fig. 1 Schematic of the preparation of the PMIA@SiO_2 separator

Experimental

Materials

PMIA solution (19.5 wt%) was purchased from Yantai Tayho Advanced Materials Co., Ltd., China, and used as received. Lithium bromide (LiBr) (purity > 99%, Sigma-Aldrich (Shanghai) Trading Co., Ltd), ethyl orthosilicate (TEOS), Tween-80 (purity > 98%, Aldrich), ethanol, propanetriol, ammonium hydroxide, and N,N-dimethylacetamide (DMAc) were supplied by Tianjin Bo Hua Chemical Industry Group Co., Ltd, China. A 1.0 mol/L $LiPF_6$ liquid electrolyte in ethylene carbonate (EC)/dimethyl carbonate (DC)/ethyl methyl carbonate (1:1:1 mass ratio) was provided by Tianjin Jin Niu Power Supply Material Co., Ltd, China. A commercial polypropylene (PP) separator was supplied by Blaze Co., Ltd, Japan.

A $LiCoO_2$ cathode (loading amount: 128 g/cm^2), natural graphite anode (loading amount: 120 g/m^2), and lithium metal sheet materials were purchased from Hefei Kejing Material Technology Co., Ltd., China.

Preparation of the PMIA Separator

Figure S1 shows the schematic for the preparation of the PMIA separator. Desired amounts of pore-making agents (3 wt% deionized water, 1 wt% LiBr, 4.8 wt% glycerol, and 8.5 wt% DMAc) were slowly added to the PMIA solution (19.5 wt%), and the solution was mechanically stirred at 25 °C to obtain a uniform casting solution. This solution was cast on a release film with an 80-μm casting knife and immediately immersed in sequential coagulation baths. After solidification, the porous separator was washed with a mixture of deionized water and ethanol (7:3 volume ratio) for 12 h to remove the residual inorganic salts (such as LiBr) and solvent.

Preparation of the PMIA@SiO_2 Separator

The schematic for the preparation of the PMIA@SiO_2 separator is shown in Fig. 1. The as-prepared PMIA separator was soaked and stirred in a mixture of Tween-80 and water with mass ratio of 1:100 for 1 h. After that, it was washed with ethanol and deionized water for three times to remove unstable residues attached and then dried in a vacuum oven at 80 °C for 30 min to obtain the PMIA@Tween separator. The PMIA@Tween and PMIA separators were soaked and stirred in a mixture of ethanol, TEOS, ammonium hydroxide and water with mass ratio of 80:1:1:3 for 2 h with stirring to obtain PMIA@SiO_2 and PMIA@SiO_2-B separators, respectively. Then, all of the separators were immersed in ethanol and sonicated for 5 min to remove unstable SiO_2 nanoparticles. The separators were further washed with ethanol several times and dried at 80 °C for 24 h before use.

Characterization

The Fourier transform infrared (FTIR) (Equinox 55, Bruker, Germany) spectra of the separators were recorded using the attenuated total reflectance (ATR) model with a resolution of 4 cm^{-1}. The surface and cross-sectional morphologies of the relevant separators were characterized using field-emission scanning electron microscopy (SEM, S-4800, Hitachi, Japan) equipped with an energy-dispersive spectrometer. The surface chemical composition of the separators was analyzed using X-ray photoelectron spectroscopy (XPS, Thermo Escalab, USA) with Al Kα excitation radiation ($h\nu = 1486.6$ eV). The contact angle of the separator was measured through contact angle analysis (DSA255, Kruss, Germany). The size and morphology of the silica nanoparticles were observed by transmission electron microscopy (TEM). The SiO_2 nanoparticles were dispersed in ethanol and dried on a carbon-coated copper grid. The mechanical properties of the separators (10 mm × 50 mm) were tested using XD-121A (Shanghai Xinrenda Instrument Co., Ltd, China) at a stretching speed of 1 mm/min. The percentage of uptake was calculated by soaking the separators into a liquid electrolyte (1 mol/L $LiPF_6$ in EC:DC:DMC = 1:1:1 mass ratio) using Eq. (1):

$$U(\%) = \frac{m_i - m_0}{m_0} \times 100\% \quad (1)$$

where m_0 and m_i are the mass of the dry separators and separators soaked in the electrolyte solution, respectively. The porosity (P) of the separators in percentage was measured by weighing and then calculated using Eq. (2):

$$P(\%) = \frac{m_t - m_s}{\rho \times V} \times 100\% \quad (2)$$

where m_t and m_s are the mass of the separators after and before impregnation with 1-butanol, respectively, and ρ and V are the density of 1-butanol and the volume of the separators, respectively. The thermal shrinkage of the separators was evaluated by the dimensional change before and after treatment under different temperatures (25, 120, 160, 200, 240 and 280 °C) for 1 h. The thermal gravimetric analysis (TGA) measurements were taken using a thermogravimetric analyzer (TGA/DSC, Mettler Toledo) over the range of 30–1000 °C under N_2 at 10 °C/min. The ionic conductivity (δ) was computed as follows:

$$\delta = \frac{d}{R_b \times A} \quad (3)$$

where R_b, d and A are the bulk impedance (ohm), thickness (cm) and effective area (cm^2), respectively. R_b was obtained by an electrochemical work station system (Parstat 2273, USA) with the assembly of stainless steel (SS)/separator-liquid electrolyte/SS. Interfacial resistance (R_{int}) was obtained by Parstat 2273 with the assembly of the lithium/separator-liquid electrolyte/lithium in alternating current (AC) impedance mode. The cycling performances and rate ability were tested with a $LiCoO_2$ cathode and lithium tablet anode, respectively. Assembled coin batteries were cycled on a cell testing system (Land CT2001A, China) under 2.5 and 4.2 V at room temperature and various discharge rates from 0.2 to 2.0 °C to test the rate capability. The cycling tests of the LIBs were galvanostatic and conducted at a discharge rate of 0.2 °C.

Results and Discussion

Morphology

Figure 2 shows the SEM images of the pristine PMIA and PMIA@SiO_2 separators. As shown in Fig. 2a, b, the pristine PMIA separator shows typically well-proportioned and a highly interconnected sponge-like cross-sectional structure that facilitates the rapid migration of lithium ions [33]. Additionally, the interconnected and tortuous pore structure can effectively prevent the penetration of lithium dendrites, which is favorable for avoiding an internal short circuit and mitigating self-discharge. After the decoration of SiO_2 nanoparticles on the separator, the SiO_2 nanoparticles agglomerated without Tween-80 as the auxiliary, as shown in Fig. 2c, d and Fig. S7. Alternatively, SiO_2 nanoparticles homogeneously attached to the pore and surface of the porous separators when Tween-80 was used (Fig. 2e, f) and the SiO_2 nanoparticle size was approximately 35 nm (Fig. S2). Tween-80

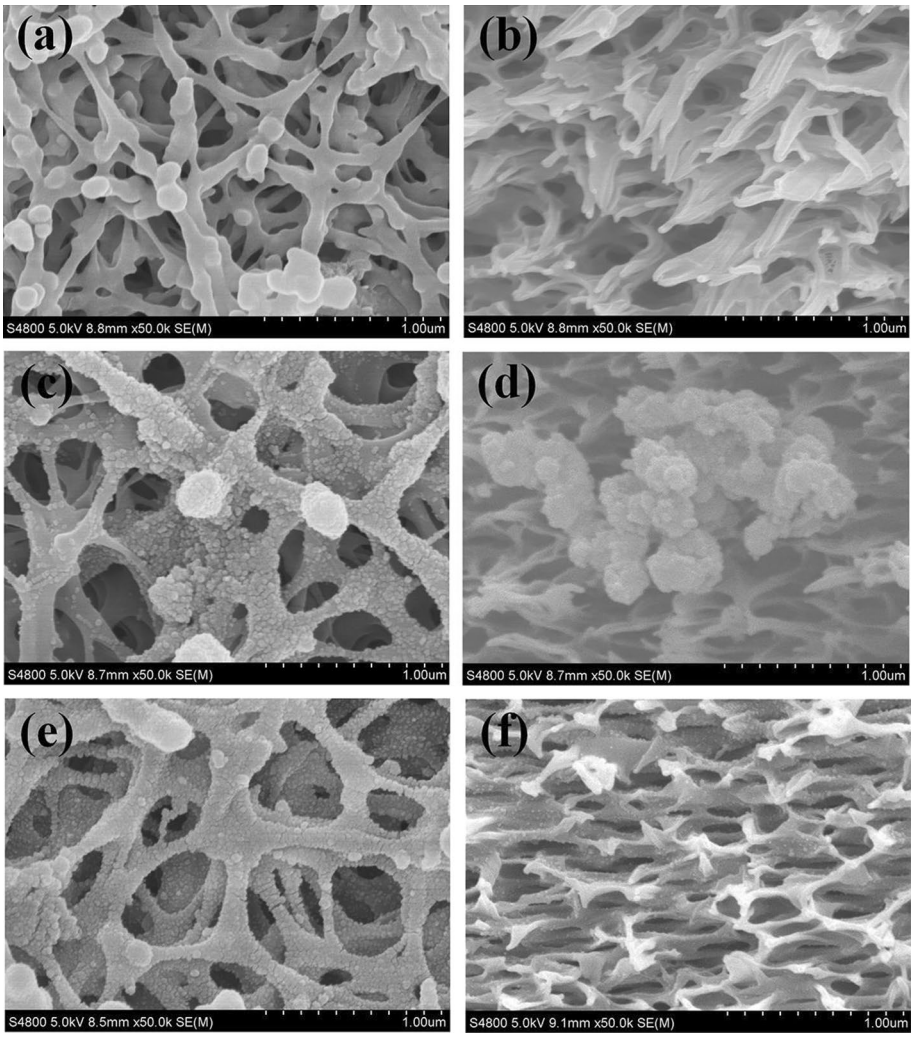

Fig. 2 SEM images of the surfaces of **a** PMIA, **c** PMIA@SiO_2-B, and **e** PMIA@SiO_2. SEM images of the cross section for **b** PMIA, **d** PMIA@SiO_2-B, and **f** PMIA@SiO_2

has good wettability for polar PMIA, which may cause Tween-80 to be uniformly adsorbed on the PMIA separator. Therefore, the large number of hydroxyl functional groups of Tween-80 assists in the uniform decoration of silica on the PMIA separator via the hydrogen bonding interaction [30]. Alternatively, Tween-80 has a long main chain and bulk side units that can generate strong steric repulsion to prevent agglomeration. Elemental mapping images (Fig. S3) show the distribution of oxygen and silicon in the PMIA@SiO_2 separator, which further proves the uniform decoration of silica nanoparticles on the PMIA separator.

Chemical Composition

XPS and FTIR (Fig. 3) were conducted to determine the composition of the PMIA@SiO_2 products. Figure 3a represents the XPS of the PMIA and PMIA@SiO_2 separators. The binding energies recorded at 104.49, 154.86, 284.63, 400.81, and 531.34 eV can be assigned to Si 2*p*, Si 2*s*, C 1*s*, N 1*s*, and O 1*s*, respectively, confirming the successful decoration of SiO_2 on the PMIA separator. Furthermore, Fig. 3b, d shows the specific O1s spectra of PMIA and PMIA@SiO_2. In Fig. 3d, the spectra deconstruct into three peaks that are centered at 532.3, 531.1, and 531.4 eV, corresponding to the C–O (carboxyl end groups of PMIA), C=O (amide groups), and Si–O, respectively [34–36]. The FTIR spectra of the PMIA and PMIA@SiO_2 separators are shown in Fig. 3c. Compared with the pristine PMIA separator, the new absorption peak at 1105 cm^{-1} of the PMIA@SiO_2 separator is assigned to the internal asymmetric stretching vibration of Si–O–Si [37], unambiguously ensuring the successful decoration of SiO_2 nanoparticles on the PMIA separator.

Mechanical Properties

The mechanical properties of battery separators are primary factors contributing to the device safety of LIBs. The mechanical properties of the PMIA and PMIA@SiO_2 separators are shown in Fig. 4. The decoration of SiO_2 nanoparticles remarkably increased the elongation at break and tensile

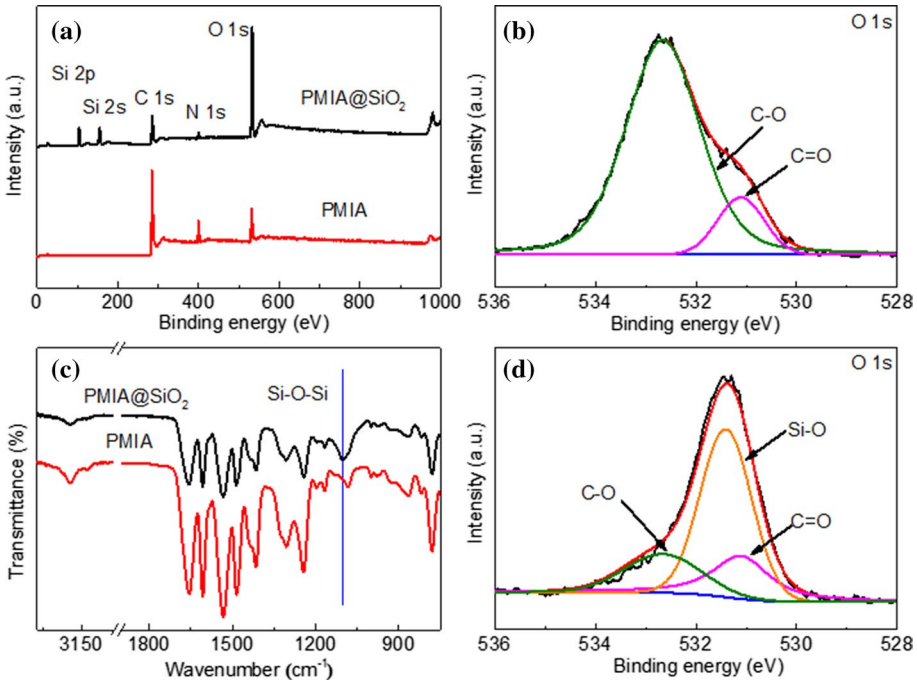

Fig. 3 XPS spectra of a full-range scan of the PMIA and PMIA@SiO_2 separators: **a** survey spectrum, O1s peak of **b** PMIA, and **d** PMIA@SiO_2. **c** FTIR spectra of the PMIA and PMIA@SiO_2 separators

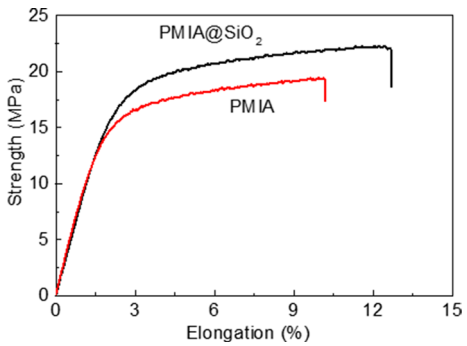

Fig. 4 Stress–strain curves of PMIA and PMIA@SiO_2

strength. Specifically, the tensile strain increased by 30% and the maximum mechanical strength improved by 16% compared with pristine PMIA, thus suggesting the robustness of the PMIA@SiO_2 separator in LIBs. According to the crazing effect, the main reason for the enhancement of mechanical strength is that the external force under attack is mainly applied to attach the SiO_2 nanoparticles rather than the polymer chain [38]. The excellent strength of the PMIA@SiO_2 separator can remarkably repress the crack-induced short circuit and restrain the penetration injury of lithium dendrites during the repeated charge–discharge process.

Thermal Stability

Thermal shrinkage of separators is an important property associated with battery electrochemical properties and safety characteristics. A superior heat-resistant separator can hinder an internal electrical short circuit and thus improve safety, especially when the batteries are used at elevated temperatures or subjected to high charge–discharge rates. Figure 5a shows the heat shrinkage testing results of PP, pure PMIA, and PMIA@SiO_2 separators. The PP separator showed an obvious shrinkage after treatment at 160 °C for 1 h, whereas the surface of the PMIA and PMIA@SiO_2 separators exerts negligible shrinkage even at 240 °C, proving that PMIA and PMIA@SiO_2 possess a high thermal stability. Figure 5b shows the thermal stability of the separator under nitrogen atmosphere. In the TGA curve, the first mass loss spans from room temperature to 100 °C, which can be ascribed to the release of H_2O adsorbed by the separator. The second mass loss at around 175 °C is caused by solvent evaporation (such as DMAc). In the third stage around 400 °C, all separators show a distinct mass loss, which might be due to the breakdown of the polymer backbone [39]. From 240 to 400 °C, the mass loss rates of the PMIA and PMIA@SiO_2 separators are 3.31% and 0.47%, respectively. The difference in mass loss may be due to the SiO_2 nanoparticles that hinder the migration of the PMIA chains, which increases the energy to trigger decomposition [24]. When the temperature increased from 400 to 1000 °C, the curve declined gently until a steady stage was reached, implying complete decomposition of the organic species and solvent in the separators and only the inorganic species (SiO_2 and coke powder) remained. Therefore, the difference between the residuals of PMIA and PMIA@SiO_2 at 1000 °C is the content of SiO_2, which is 4.24%. The above results confirm that the PMIA@SiO_2 separator has outstanding

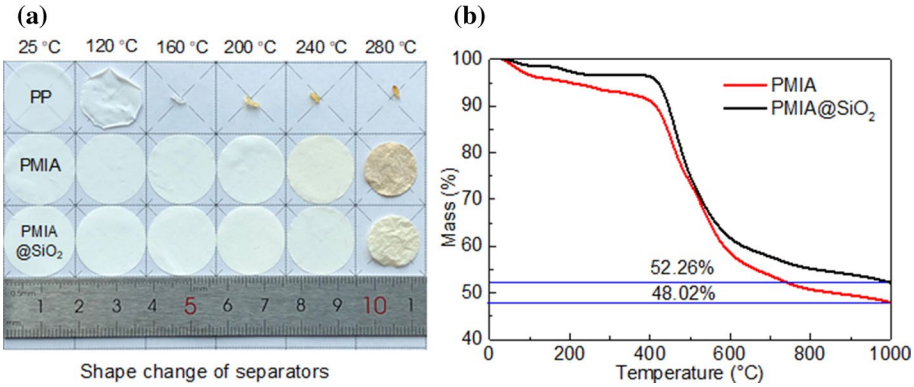

Fig. 5 **a** The shape change of PP, PMIA, and PMIA@SiO_2 separators at different temperatures and **b** thermograms of the PMIA and PMIA@SiO_2 separators

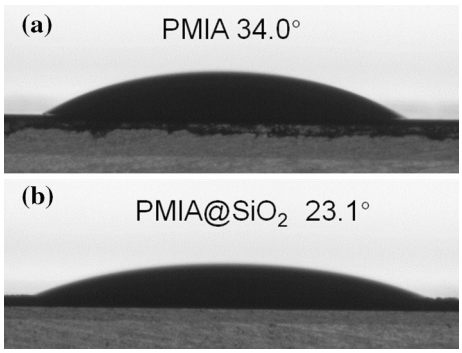

Fig. 6 Contact angles of the **a** PMIA and **b** PMIA@SiO_2 separators

Table 1 Physical properties of the separators

Separator	Uptake (%)	Porosity (%)
PMIA	149.28	65.74
PMIA@SiO_2	208.15	65.51

thermal stability, which can effectively prevent short circuits induced by the dimensional reduction of separators.

Wettability and Liquid Electrolyte Uptake

The wettability of separators in the electrolyte solution was evaluated, and the results are shown in Fig. 6. The pristine PMIA separator shows an electrolyte contact angle of 34.0°, indicating weak affinity for liquid electrolytes. After the decoration of SiO_2 nanoparticles, the affinity between the PMIA@SiO_2 separators and electrolyte increases, as evidenced by the contact angle (23.1°) of the PMIA@SiO_2 separator, which can accelerate electrolyte diffusion [40].

The electrolyte uptake and porosity data of the separators are summarized in Table 1. The liquid electrolyte uptake of the PMIA@SiO_2 separator increases from 149 to 208% compared with that of the pristine PMIA separator for the following reasons. The addition of SiO_2 can increase the surface roughness of the PMIA@SiO_2 separator, which improves the absorption of the electrolyte. Alternatively, SiO_2 nanoparticles with high surface areas increase the liquid electrolytes absorption of separator [41]. The pore size distribution of the PMIA and PMIA@SiO_2 separators was obtained by mercury intrusion porosimetry (Fig. S4). The majority of the pore sizes was between 0.8 and 1.0 μm, which benefits to preventing the penetration of lithium dendrites and electrode component particles [42].

Electrochemical Properties

The ionic conductivity of the separator is a key parameter determining the electrochemical performance of LIBs, which is mainly affected by two factors: (1) the high liquid electrolyte uptake, which increases the ionophores of the separator and (2) the interconnected porous structure of the separator, which facilitates lithium-ion migration. As shown in the electrochemical impedance spectroscopy (EIS) spectra in Fig. 7a, the bulk resistances (R_b) of the PMIA and PMIA@SiO_2 separators are 2.7 and 1.9 Ω, respectively. The calculated ionic conductivity follows the sequence of PMIA@SiO_2 separator (0.75 mS/cm) > PMIA separator (0.52 mS/cm). Given its high porosity and electrolyte uptake, the PMIA@SiO_2 separator could absorb more electrolytes, which help the fluent flow of Li ions through the pore channels in the PMIA@SiO_2 separator.

Interfacial resistance is another key parameter determining the electrochemical performance of LIBs. The interfacial resistance of the lithium/separator-liquid electrolyte/lithium coin cells is shown in Fig. 7c. The average initial interface resistance of LIBs assembled with the PMIA@SiO_2 separator is 75 Ω, which is lower than that of the LIBs assembled with the pristine PMIA separator (100 Ω). It shows that the PMIA@SiO_2 separator allows easy passage of the charge carriers. One reason is that the PMIA@SiO_2 separator exhibits electrolyte wettability and enhances electrolyte uptake (Table 1). Another reason is that the Si–O units exposed to the PMIA@SiO_2 separator can act as Lewis acid sites to capture electrolyte anions, thus inhibiting the oxidative decomposition of lithium salt anions, which can

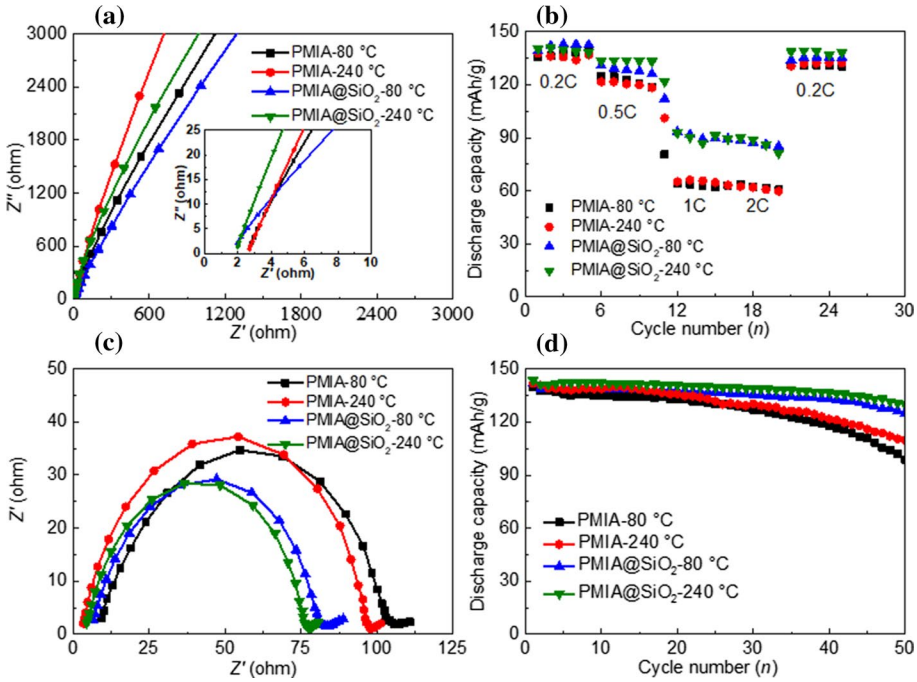

Fig. 7 **a** AC impedance spectra of liquid electrolyte-soaked PMIA and PMIA@SiO_2 separators at different temperatures. **b** Rate capability of the LIBs with the PMIA and PMIA@SiO_2 separators at different temperatures. **c** Interfacial resistance of the PMIA and PMIA@SiO_2 separators in Li/separator-liquid electrolyte/Li cells at different temperatures. **d** Cycle performance of LIBs with the PMIA and PMIA@SiO_2 separators at different temperatures

further stabilize the interface [43, 44]. The *I–V* curves of the separators are shown in Fig. S5. The current of the PMIA and PMIA@SiO_2 separators abruptly increased at approximately 4.9 V versus Li^+/Li, owing to the electrochemical decomposition of electrolyte ($LiPF_6$) at this potential, and also implying that 4.9 V is the electrochemical window of cells. However, a working potential between 1.8 and 3.5 V is actually used for LIBs [44, 45], indicating that the PMIA and PMIA@SiO_2 separators have a good potential for application in LIBs.

Coin cells were constructed using a $LiCoO_2$ cathode, Li metal anode, and various separators to investigate the application of the PMIA@SiO_2 separator in LIBs. Figure 7c shows the charge–discharge measurements at different current densities (0.2–2 °C) of coin cells with different separators. The coin cells with the PMIA@SiO_2 separator have a higher discharge capacity than the pristine PMIA separator, which is ascribed to the low interfacial resistance between the electrodes and PMIA@SiO_2 separator as well as the high ionic conductivity. Figure 7d shows the cycling stability of the coin cells with the pristine PMIA and PMIA@SiO_2 separators through the galvanostatic charge–discharge test after 50 cycles at 0.2 C. The cell with the PMIA@SiO_2 separator shows the highest discharge capacity of 142.1 mAh/g (Fig. S6) after 50 cycles with a capacity retention of 88.1%. This result clearly indicates that the LIBs with the PMIA@SiO_2 separator have better cycle stability than the pristine PMIA separator, which can be attributed to the higher ionic conductivity and lower interfacial resistance for the former than the latter. The PMIA and PMIA@SiO_2 separators were annealed at 240 °C prior to assembly to verify the stability of batteries assembled with these separators. The $LiCoO_2$/Li cell using the separator with high-temperature treatment (240 °C) shows better performance than the separator with treatment less than 80 °C, which may be attributed to the removing of trace amounts of moisture and residual solvent in the separator that has been heat treated at high temperature [46]. Therefore, the PMIA@SiO_2 composite separator is a potential candidate for LIBs with a high-safety requirement.

Conclusion

In summary, a nano-silica-decorated PMIA separator with good mechanical strength (improved by 16% compared with pristine PMIA) and wettability toward the electrolyte was successfully prepared. The decorating process is binder-free, and SiO_2 nanoparticles uniformly decorated the surfaces and internal pore walls of the porous separators, which were helpful to improve the mechanical strength and wettability of the separator. The as-prepared PMIA@SiO_2 separator showed high ionic conductivity (0.75 mS/cm) as well as low interfacial impedance, which were crucial for improving the cycling stability of LIBs. Furthermore, the LIBs assembled with the PMIA@SiO_2 separator exerted a capacity retention of 88.1% after 50 cycles. In addition, the PMIA@SiO_2 separator retains good performance in LIBs even after a high-temperature treatment. Therefore, the nano-silica-decorated PMIA separator is a potential candidate for application in LIBs.

Acknowledgements This study was supported by National Science and Technology Major Project (No. 2016ZX02025-004-006) and Science and Technology Project of China National Offshore Oil Corporation (No. CNOOC-KJ 135 ZDXM 35 TJY 009-2017).

References

1. Jiang ZY, Xie HQ, Wang SQ et al (2018) Perovskite membranes with vertically aligned microchannels for all-solid-state lithium batteries. Adv Energy Mater 8(27):1801433
2. Chen XZ, He WJ, Ding LX et al (2019) Enhancing interfacial contact in all solid state batteries with a cathode-supported solid electrolyte membrane framework. Energy Environ Sci 12(3):938–944
3. Lagadec MF, Zahn R, Wood V (2019) Characterization and performance evaluation of lithium-ion battery separators. Nat Energy 4(1):16–25
4. Zhao HJ, Deng NP, Yan J et al (2019) Effect of OctaphenylPolyhedral oligomeric silsesquioxane on the electrospun poly-*m*-phenylene isophthalamid separators for lithium-ion batteries with high safety and excellent electrochemical performance. Chem Eng J 356:11–21
5. Zhang H, Lin CE, Zhou MY et al (2016) High thermal resistance polyimide separators prepared via soluble precusor and non-solvent induced phase separation process for lithium ion batteries. Electrochim Acta 187:125–133
6. Xiang HF, Chen JJ, Li Z et al (2011) An inorganic membrane as a separator for lithium-ion battery. J Power Sour 196(20):8651–8655
7. Jiang ZY, Wang SQ, Chen XZ et al (2020) Lithium-metal batteries: tape-casting $Li_{0.34}$ $La_{0.56}TiO_3$ ceramic electrolyte films permit high energy density of lithium–metal batteries. Adv Mater 32(6):2070045
8. Zhang H, Zhang Y, Yao ZK et al (2016) Novel configuration of polyimide matrix-enhanced cross-linked gel separator for high performance lithium ion batteries. Electrochim Acta 204:176–182
9. Subramania A, Kalyana Sundaram NT, Sathiya Priya AR et al (2007) Preparation of a novel composite micro-porous polymer electrolyte membrane for high performance Li-ion battery. J Membr Sci 294(1–2):8–15
10. Wang LY, Deng NP, Ju JG et al (2019) A novel core-shell structured poly-*m*-phenyleneisophthalamide@polyvinylidene fluoride nanofiber membrane for lithium ion batteries with high-safety and stable electrochemical performance. Electrochim Acta 300:263–273
11. Wang ZH, Xiang HF, Wang LJ et al (2018) A paper-supported inorganic composite separator for high-safety lithium-ion batteries. J Membr Sci 553:10–16
12. Kang WM, Deng NP, Ma XM et al (2016) A thermostability gel polymer electrolyte with electrospun nanofiber separator of organic F-doped poly-*m*-phenylene isophthalamide for lithium-ion battery. Electrochim Acta 216:276–286
13. Chen WW, Weng WG (2016) Ultrafine lauric–myristic acid eutectic/poly (meta-phenylene isophthalamide) form-stable phase change fibers for thermal energy storage by electrospinning. Appl Energy 173:168–176
14. Wang XR, Si Y, Wang XF et al (2013) Tuning hierarchically aligned structures for high-strength PMIA–MWCNT hybrid nanofibers. Nanoscale 5(3):886–889
15. Wang T, He XP, Li Y et al (2018) Novel poly(piperazine-amide) (PA) nanofiltration membrane based poly(*m*-phenylene isophthalamide) (PMIA) hollow fiber substrate for treatment of dye solutions. Chem Eng J 351:1013–1026
16. Zhang H, Zhang Y, Xu TG et al (2016) Poly(*m*-phenylene isophthalamide) separator for improving the heat resistance and power density of lithium-ion batteries. J Power Sour 329:8–16
17. Lee JH, Manuel J, Liu Y et al (2016) High temperature resistant electrospun nanofibrous meta-aramid separators for lithium ion batteries. J Nanosci Nanotechnol 16(10):10724–10729
18. Zhai YY, Wang N, Mao X et al (2014) Sandwich-structured PVdF/PMIA/PVdF nanofibrous separators with robust mechanical strength and thermal stability for lithium ion batteries. J Mater Chem A 2(35):14511–14518
19. Xiao K, Zhai YY, Yu JY et al (2015) Nanonet-structured poly(*m*-phenylene isophthalamide)–polyurethane membranes with enhanced thermostability and wettability for high power lithium ion batteries. RSC Adv 5(68):55478–55485
20. Yang CL, Li ZH, Li WJ et al (2015) Batwing-like polymer membrane consisting of PMMA-grafted electrospun PVdF–SiO_2 nanocomposite fibers for lithium-ion batteries. J Membr Sci 495:341–350
21. Cao CY, Tan L, Liu WW et al (2014) Polydopamine coated electrospun poly(vinyldiene fluoride) nanofibrous membrane as separator for lithium-ion batteries. J Power Sour 248:224–229
22. Zhao HJ, Kang WM, Deng NP et al (2020) A fresh hierarchical-structure gel poly-*m*-phenyleneisophthalamide nanofiber separator assisted by electronegative nanoclay-filler towards high-performance and advanced-safety lithium-ion battery. Chem Eng J 384:123312
23. Li Y, of Chemical Engineering School of Chemical Engineering and Technology Tianjin University Tianjin China SKL (2019) A sandwich-structure composite membrane as separator with high wettability and thermal properties for advanced lithium-ion batteries. Int J Electrochem Sci 7088–7103
24. Li YF, Ma XM, Deng NP et al (2017) Electrospun SiO_2/PMIA nanofiber membranes with higher ionic conductivity for high temperature resistance lithium-ion batteries. Fibers Polym 18(2):212–220
25. Jeon KS, Nirmala R, Navamathavan R et al (2014) The study of efficiency of Al_2O_3 drop coated electrospun meta-aramid nanofibers as separating membrane in lithium-ion secondary batteries. Mater Lett 132:384–388
26. Zhao HJ, Deng NP, Kang WM et al (2020) The significant effect of octa(aminophenyl)silsesquioxane on the electrospun ion-selective and ultra-strong poly-*m*-phenyleneisophthalamide separator for enhanced electrochemical performance of lithium-sulfur battery. Chem Eng J 381:122715
27. Yang CL, Liu HY, Xia QL et al (2014) Effects of SiO_2 nanoparticles and diethyl carbonate on the electrochemical properties of a fibrous nanocomposite polymer electrolyte for rechargeable lithium batteries. Arab J Sci Eng 39(9):6711–6720
28. Park JH, Cho JH, Park W et al (2010) Close-packed SiO_2/poly(methyl methacrylate) binary nanoparticles-coated polyethylene separators for lithium-ion batteries. J Power Sour 195(24):8306–8310
29. Wang Y, Wang SQ, Fang JQ et al (2017) A nano-silica modified polyimide nanofiber separator with enhanced thermal and

wetting properties for high safety lithium-ion batteries. J Membr Sci 537:248–254
30. Zenerino A, Amigoni S, Taffin de Givenchy E et al (2013) Homogeneous dispersion of SiO_2 nanoparticles in an hydrosoluble polymeric network. React Funct Polym 73(8):1065–1071
31. Qi DM, Gao F, Chen ZJ et al (2017) Preparation of composite films with controlled dispersion state of SiO2 nanoparticles by using polymer/SiO2 nanocomposite particles. Colloids Surf A Physicochem Eng Asp 523:106–117
32. Gowri VS, Almeida L, Amorim T et al (2012) Novel copolymer for SiO_2 nanoparticles dispersion. J Appl Polym Sci 124(2):1553–1561
33. Zhang JJ, Liu ZH, Kong QS et al (2013) Renewable and superior thermal-resistant cellulose-based composite nonwoven as lithium-ion battery separator. ACS Appl Mater Interfaces 5(1):128–134
34. Montes-Morán MA, Paredes JI, Martínez-Alonso A et al (2002) Surface characterization of PPTA fibers using inverse gas chromatography. Macromolecules 35(13):5085–5096
35. Cheng DK, Dai XH, Chen L et al (2020) Thiol–yne click synthesis of polyamide–amine dendritic magnetic halloysite nanotubes for the efficient removal of Pb(II). ACS Sustain Chem Eng 8(2):771–781
36. Sa RN, Yan WL et al (2015) Improved adhesion properties of poly-p-phenyleneterephthamide fibers with a rubber matrix via UV-initiated grafting modification. RSC Adv 5(114):94351–94360
37. Meng JK, Cao Y, Suo Y et al (2015) Facile fabrication of 3D SiO2@Graphene aerogel composites as anode material for lithium ion batteries. Electrochim Acta 176:1001–1009
38. Li WL, Xing YJ, Wu YH et al (2015) Study the effect of ion-complex on the properties of composite gel polymer electrolyte based on Electrospun PVdF nanofibrous membrane. Electrochim Acta 151:289–296
39. Villar-Rodil S, Paredes JI, Martínez-Alonso A et al (2001) Atomic force microscopy and infrared spectroscopy studies of the thermal degradation of nomex aramid fibers. Chem Mater 13(11):4297–4304
40. Wang ZY, Guo FL, Chen C et al (2015) Self-assembly of PEI/SiO_2 on polyethylene separators for Li-ion batteries with enhanced rate capability. ACS Appl Mater Interfaces 7(5):3314–3322
41. Yanilmaz M, Lu Y, Dirican M et al (2014) Nanoparticle-on-nanofiber hybrid membrane separators for lithium-ion batteries via combining electrospraying and electrospinning techniques. J Membr Sci 456:57–65
42. Zhang SS (2007) A review on the separators of liquid electrolyte Li-ion batteries. J Power Sources 164(1):351–364
43. Fu D, Luan B, Argue S et al (2012) Nano SiO_2 particle formation and deposition on polypropylene separators for lithium-ion batteries. J Power Sour 206:325–333
44. Yanilmaz M, Dirican M, Zhang XW (2014) Evaluation of electrospun SiO2/nylon 6,6 nanofiber membranes as a thermally-stable separator for lithium-ion batteries. Electrochim Acta 133:501–508
45. Fan XY, Liu B, Liu J et al (2020) Battery technologies for grid-level large-scale electrical energy storage. Trans Tianjin Univ 26(2):92–103
46. Schweiger HG, Multerer M, Wietelmann U et al (2005) NMR determination of trace water in lithium salts for battery electrolytes. J Electrochem Soc 152(3):A622

Zan Chen is a Senior Engineer and received his PhD. from Dalian University of Technology in 2009. Currently, he is director of Membrane and Membrane Process Laboratory in CenerTech Tianjin Chemical Research and Design Institute Co., Ltd. And he is also a leader of innovation team in key areas of Tianjin Innovation Talent Promotion Plan. He has received a number of awards including the CNOOC Group Company "Make Individuals (2015), the second prize of Beijing Science and Technology Award (2003), the second prize of CNOOC group's technology invention (2017), the second prize of Science and Technology of CNOOC Tianjin Branch (2017), the second prize of CNOOC Development Scientific and Technological Achievements (2018), the third prize of CNOOC Development Achievement Transformation (2019). He has authored or co-authored over 10 papers in peer-reviewed journals. He is interested in molecular sieve composite membrane and membrane related to CO_2 removal from natural gas.

Yanlei Su is associate Prof. at School of Chemical Engineering of Tianjin University. He graduated from Chinese Academy of Sciences with a doctorate in chemical engineering in 2003. He has received a number of awards including the National Outstanding Doctoral Dissertation Nomination Award (2005), the second prize of Beijing Science and Technology Award (2003), the dean's excellence award of Chinese Academy of Sciences (2003), the second prize of China Association for Analysis and Testing Science and Technology Award (CAIA Award) (2003). He has authored or co-authored over 50 papers in peer-reviewed journals and has been invited as a speaker at national and international meetings on related fields. He is interested in the science and technology of membrane separation, focusing on permeable bionic membrane, anti-fouling membrane, stimulus response (intelligent) membrane, controllable adsorption-desorption membrane, etc.